Article

Investigation on Development of Sliding Mode Controller for Constant Power Loads in Microgrids

Eklas Hossain [1], Ron Perez [2], Sanjeevikumar Padmanaban [3,*] and Pierluigi Siano [4]

[1] Department of Electrical Engineering & Renewable Energy, Oregon Tech, Klamath Falls, OR 97601, USA; eklas.hossain@oit.edu
[2] Department of Mechanical Engineering, University of Wisconsin-Milwaukee, Milwaukee, WI 53211, USA; perez@uwm.edu
[3] Department of Electrical and Electronics Engineering, University of Johannesburg, Auckland Park, South Africa
[4] Department of Industrial Engineering, University of Salerno, Salerno 84084, Italy; psiano@unisa.it
* Correspondence: sanjeevi_12@yahoo.co.in; Tel.: +27-79-219-9845

Abstract: To implement renewable energy resources, microgrid systems have been adopted and developed into the technology of choice to assure mass electrification in the next decade. Microgrid systems have a number of advantages over the conventional utility grid systems, however, it faces severe instability issues due to continually increasing constant power loads. To improve the stability of the entire system, load side compensation technique is chosen because of its robustness and cost effectiveness. In this particular occasion, a sliding mode controller is developed for microgrid system in the presence of CPL to assure certain control objective of keeping the output voltage constant at 480V. After that, the robustness analysis of the sliding mode controller against parametric uncertainties is presented. The sliding mode controller robustness against parametric uncertainties, frequency variations, and additive white Gaussian noise (AWGN) are illustrated in this paper. Later, the performance of the PID and sliding Mode controller is compared in case of nonlinearity, parameter uncertainties, and noise rejection to justify the selection of Sliding Mode controller over PID controller. All the necessary calculations are reckoned mathematically and results are verified in the virtual platform such as MATLAB/Simulink with the appreciable outcome.

Keywords: sliding mode control; constant power load; negative incremental impedance; robustness analysis; chattering reduction; microgrid stability; noise rejection

1. Introduction

Microgrid systems deal with several kinds of loads. Based on load function, electrical loads can be classified into two main types: Constant Impedance Loads (CIL) and Constant Power Loads (CPL). Traditional loads are of the former category, e.g. incandescent lighting, induction motors, resistive heating, etc. These typically present a constant impedance to the electrical network and are modeled by a resistor or resistor- inductor combination. Since the early days of electrical energy, these have been the only loads which grid operators have faced. However, with the arrival of modern micro/power electronics, non-traditional loads have appeared which do not behave in a similar way in power systems. Non-traditional loads such as switch-mode supplies with regulation, back-to-back converters, electric motor drives, and power electronic circuits fall into this second category called constant power loads. The typical V-I characteristics of constant voltage load (CVL) and constant power load (CPL) are presented below in figure 1. Today's devices require strict control and regulation of operating parameters to function properly. Strictly regulated point-of-load converters mean that the power output of these devices remains constant, even though the input voltage changes. The use of active rectifiers is becoming the preferred interface for loads in distribution systems with the increasing concern on power quality issues [1, 2].

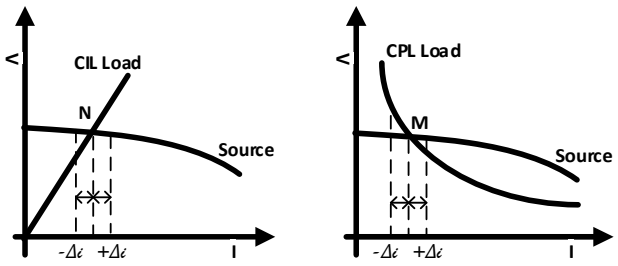

Fig 1: Typical V-I characteristics of (a) Constant Voltage Load (CVL) or Constant Impedance Load, (b) Constant Power Load [4].

As electronic loads increase, the proportion of CPLs in the overall load will rise. This change in proportion brings about problems in system stability due to CPL characteristics [3, 4]. While these problems were known before, the fraction of CPL was too small to demand much concern. With changes occurring worldwide in electrical energy distribution and consumption, these problems now require further investigation. Since the last decade, a great deal of research has been done to overcome the CPL instability issue [5]. But, none of it is able to provide the comprehensive solution of this phenomenon with sensitivity analysis of the entire system and appropriate compensation technique for microgrid application. Therefore, more research is still required in this field [6, 7].

To improve the stability scenario of the microgrid system, several linear and nonlinear control techniques have already been adopted [8, 9]. Besides that, researchers and professionals have been conducting cutting-edge research to enhance the system stability around the world [10]. In the case of DC microgrid, a number of researchers are reviewed at [11-13]. After investigating a number of research works on stability issues on a microgrid, where the majority of the loads is installed with CPL, we come to the conclusion that CPL instability compensation techniques can be classified into three groups. These are (i) feeder side compensation, (ii) compensation by adding intermediate circuitry, (iii) load side compensation [14]. It is evident if CPL compensation is done in load side, the system doesn't experience the effect of constant power loads. The load side compensation technique offers better robustness as well as cost effectiveness. Hence, in this paper, Sliding Mode Control (SMC) technique will be implemented in the case of load side compensation for CPL instability in microgrid systems. Before this, some research works have been accomplished by the sliding mode control technique. With large systems, the stability characteristics become more difficult to establish. To use the original, non-linear models of the system, sliding mode control has been implemented in DC microgrids [15-17] by finding a sliding surface and using a discontinuous sliding mode controller to improve voltage stability. In like manner, a non-linear sliding surface is proposed by the two researchers from the Indian Institute of Technology Jodhpur, Suresh Singh and Deepak Fulwani at [18] to mitigate CPL instability. Their proposed non-linear surface confirmed that the constant power was maintained, in practice, by the converter. Thus, the proposed controller was necessarily able to mitigate the CPL's oscillating effect of tightly regulated POLs and assure the stable operation of DC microgrid under a number of disturbances. Apart from that, researchers, Aditya R. Gautam et al presented, at [19], a robust sliding mode control technique to investigate CPL instability. After that, in [20], Vinicius Stramosk and Daniel J. Pagano proposed a novel Sliding Mode Controller to control the DC bus voltage precisely. In the case of AC microgrid, a number of researchers are reviewed at [21-23]. Using all the background knowledge of this research, the cardinal objective of this paper is to develop a novel sliding mode controller for microgrids with constant power loads [24, 25].

In this paper, section 2, Constant Power Load (CPL) instability is presented with necessary illustration. After that, in section 3, the Sliding Mode Control (SMC) technique is introduced. In this section, the control principle of SMC, chattering, chattering reduction, advantages of SMC, controller design, and control objectives are delineated with necessary equations and depictions. In section 4,

the robustness analysis of SMC is presented. After that, in section 5, results and simulations are illustrated in the case of a number of system parameters between robustness analysis against parametric variation and robustness analysis against parametric uncertainties, frequency variation and additive Gaussian noise using SMC control technique based on boundary condition.

The contributions of this paper are as follows: development of sliding mode controller for microgrids with constant power load to assure control objectives/desired output. The robustness of the sliding mode controller against parametric uncertainties will be presented in this paper. Besides that, the sliding mode controller robustness against Parametric Uncertainties, Frequency Variations and Additive white Gaussian Noise (AWGN) will be illustrated. Finally, the performance of the PID and Sliding Mode Control technique will be compared to microgrid output voltage in case of nonlinearity, parameter uncertainties, and noise rejection.

2. Modeling of microgrid with CPL

The small signal equivalent model of the microgrid is represented in figure 2, where the combination of Req and Leq is the line impedance or generator impedance and Ceq represents the filter capacitance.

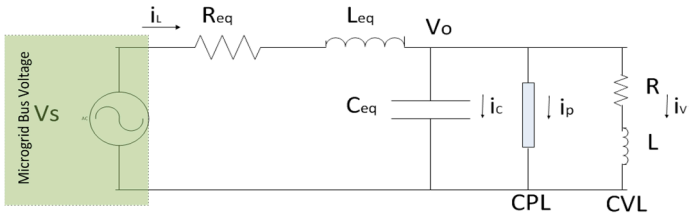

Figure 2: Equivalent Circuit of AC Microgrid with CPL & CVL [26].

For the ease of controlling uncompensated nonlinear systems and presenting a detailed analysis of state variables to implement the advanced nonlinear control algorithms, we have derived d-q axis modeling of the designed system. The equivalent d-q axis model circuit is represented in figure 3(a) and 3(b). When we consider line frequency is 60 Hz, then ω (speed term) becomes static. However, in practical cases, line frequency always fluctuates which depends on various characteristics of the system. So, in those cases, ω (speed term) becomes dynamic and nonlinear.

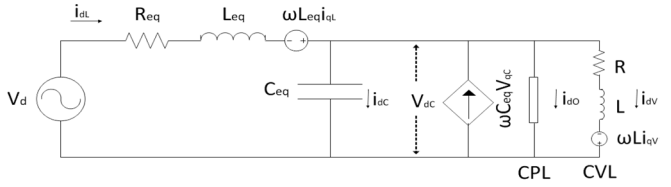

(a) d-axis model of Microgrid

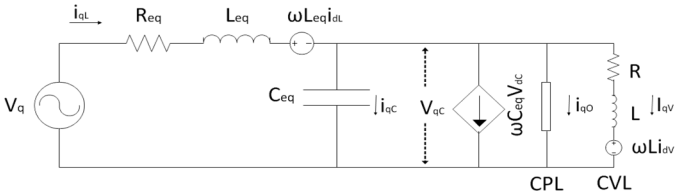

(b) q-axis model of Microgrid

Figure 3: d-q axis model of microgrid system

D-q transformed state equations can be represented by figure 3 as

$$\begin{bmatrix} \frac{di_{dL}}{dt} \\ \frac{di_{qL}}{dt} \\ \frac{dV_{dC}}{dt} \\ \frac{dV_{qC}}{dt} \\ \frac{di_{qV}}{dt} \\ \frac{di_{qV}}{dt} \end{bmatrix} = \begin{bmatrix} \omega i_{qL} - \frac{R_1}{L_1} i_{dL} - \frac{V_{dc}}{L_1} + \frac{V_d}{L_1} \\ -\omega i_{dL} - \frac{R_1}{L_1} i_{qL} - \frac{V_{qc}}{L_1} + \frac{V_q}{L_1} \\ \omega V_{qC} + \frac{1}{C} i_{dL} - \frac{1}{C} \frac{P_O}{V_{dC}} - \frac{1}{C} i_{dV} \\ -\omega V_{dC} + \frac{1}{C} i_{qL} - \frac{1}{C} \frac{P_O}{V_{qc}} - \frac{1}{C} i_{qV} \\ \omega i_{qV} + \frac{1}{L} V_{dC} - \frac{R}{L} i_{dV} \\ -\omega i_{dV} + \frac{1}{L} V_{qC} - \frac{R}{L} i_{qV} \end{bmatrix} \quad (1)$$

Using the equation 1, in figure 4, the bus voltage instability of d-axis due to the constant power loads is presented schematically. In this case, an abrupt and random change is observed in d-axis bus voltage.

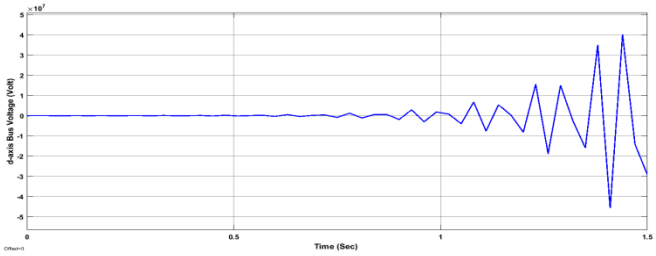

Figure 4: d-axis bus voltage instability due to CPL.

In this sequence, at figure 5, the bus voltage instability of q-axis due to the constant power loads is presented. Like the d-axis bus voltage, the exponentially increased signal and random oscillation are also demonstrated in the case of the q-axis bus voltage.

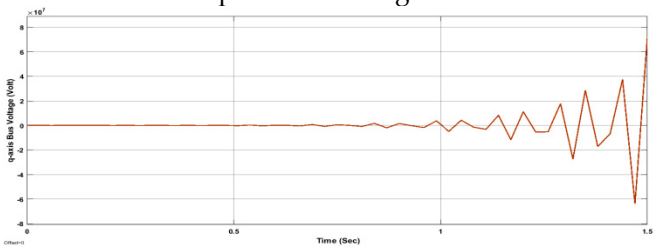

Figure 5: q-axis bus voltage instability due to CPL.

In the following illustration at figure 6, the entire design of the microgrid arrangement loaded with CPLs is depicted for d-q representation. The figure exhibits the undamped oscillation due to the perturbation created by the CPL loads in case of microgrid d axis and q axis bus voltage. This disturbance in both of the output voltages leads to the undesired voltage collapse in the microgrid system.

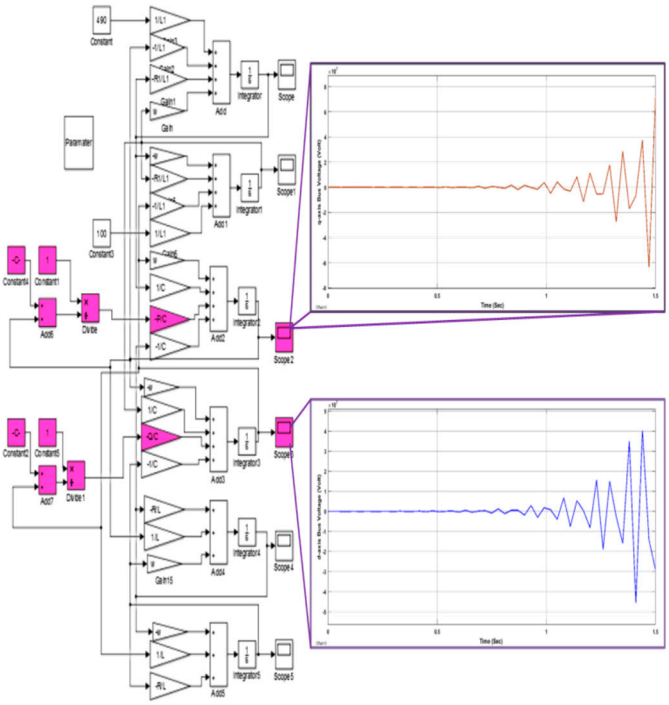

Figure 6: The schematic diagram of a microgrid system, which has been made unstable by a CPL while control inputs are absent.

To mitigate this perturbation due to CPL loads, the load side compensation technique is reasonably adopted rather than the feeder side compensation and the intermediate circuitry compensation technique. In the load side compensation technique, necessary manipulation is made in load side of the system so that the system doesn't experience the effect of constant power loads. To clarify this technique, the real power compensation and reactive power compensation technique are modeled below schematically in figure 7 and figure 8.

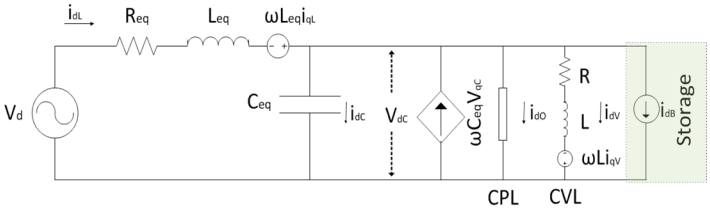

Figure 7: d-axis model of the load side real power compensation method.

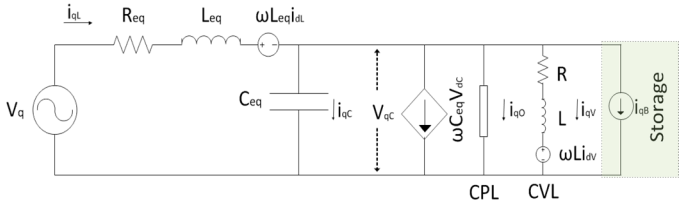

Figure 8: q-axis model of the load side reactive power compensation method.

From the above dq-axis modeling, the combined state space equation of the adopted load side compensation technique is presented in equation 2.

Preprints (www.preprints.org) | NOT PEER-REVIEWED | Posted: 18 May 2017 doi:10.20944/preprints201705.0137.v1

Peer-reviewed version available at Energies 2017, 10, 1086; doi:10.3390/en10081086

$$\begin{bmatrix} \frac{di_{dL}}{dt} \\ \frac{di_{qL}}{dt} \\ \frac{dV_{dC}}{dt} \\ \frac{dV_{qC}}{dt} \\ \frac{di_{qV}}{dt} \\ \frac{di_{qV}}{dt} \end{bmatrix} = \begin{bmatrix} \omega i_{qL} - \frac{R_1}{L_1} i_{dL} - \frac{V_{dc}}{L_1} + \frac{V_d}{L_1} \\ -\omega i_{dL} - \frac{R_1}{L_1} i_{qL} - \frac{V_{qc}}{L_1} + \frac{V_q}{L_1} \\ \omega V_{qC} + \frac{1}{C} i_{dL} - \frac{1}{C} \frac{P_O}{V_{dC}} - \frac{1}{C} i_{dV} - \frac{1}{C} i_{dB} \\ -\omega V_{dC} + \frac{1}{C} i_{qL} - \frac{1}{C} \frac{Q_O}{V_{qc}} - \frac{1}{C} i_{qV} - \frac{1}{C} i_{qB} \\ \omega i_{qV} + \frac{1}{L} V_{dC} - \frac{R}{L} i_{dV} \\ -\omega i_{dV} + \frac{1}{L} V_{qC} - \frac{R}{L} i_{qV} \end{bmatrix} \quad (2)$$

3. Sliding mode controller design

Sliding mode control, commonly known as SMC technique, is an advanced nonlinear control strategy that features salient properties of accuracy, robustness, and easy tuning and adjusts the system dynamics by the function of discontinuous control signal, forcing the system output to 'slide' along with sliding surface or a defined cross-section of the system's nominal behavior [27]. Here, the state feedback control law, a discontinuous function of time, can shift from one structure to another (in a continuous manner) based on the prevailing location in the space. Therefore, the SMC can be defined as a variable structured control technique. The certain operation mode of the system, as it slides along the predefined boundaries of the control structures, is called the sliding mode. Besides that, the geometrical locus, necessarily consisting of the boundaries, is said to be the sliding surface of the system. Here, Figure 9 depicts an instance of the trajectory of a certain system regarding the SMC technique. In this illustration, the sliding surface is defined by, s= 0, and, in this occasion, the sliding mode starts after a finite time while the system trajectories have come to the specified surface.

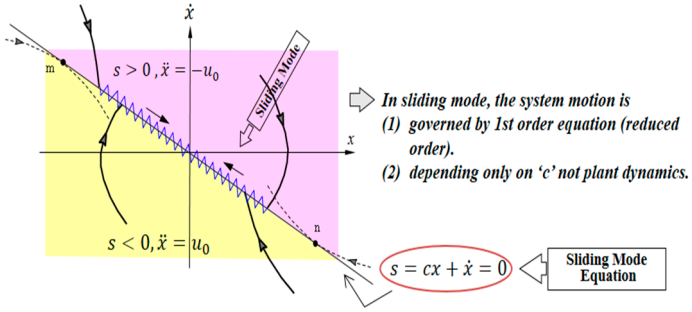

Figure 9: Schematic representation of sliding mode control scheme [28].

- State trajectories are toward the switching line s=0
- State trajectories cannot leave and belong to the switching line s=0
- After sliding mode starts, further motion is governed by $s = cx + \dot{x} = 0$

3.1. Chattering:

The absolute sliding mode remains only while the state trajectory x (t) of the controlled plant complies with the coveted trajectory at each t≥t_1 for some value of t_1 [29]. Here, it may need the infinitely rapid switching. But, in the case of the practical systems, the switching controller does have a number of inadequacies that actually confines switching up to a definite frequency. In this occasion, then the representative point oscillates within a predefined neighborhood of the switching surface. In particular, this kind of oscillation is said to be the chattering [30]. This phenomenon is presented in figure 10.

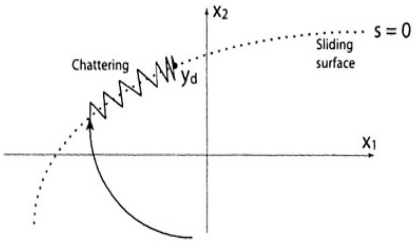

Figure 10: Chattering as a result of imperfect control switching [31].

3.2. Chattering Reduction:

Control laws which satisfying sliding condition (The simplified 1st order problem of keeping the scalars at zero can be achieved by choosing the control law u such that outside of s (t) as1/2 d/dt s^2≤-η|s|, where η is a strictly positive constant) and lead to "perfect" tracking in the face of model uncertainty, are discontinuous across the surface S (t), thus causing control chattering. Chattering is undesirable for the designers because it demands extremely high control activity, and furthermore it involves with the high-frequency dynamics which is neglected in the course of modeling. Chattering must be reduced (eliminated) for the controller to perform properly. This can be achieved by smoothing out the control discontinuity in a thin boundary layer neighboring the switching surface in equation (3)

$$B(t)=\{x,|s(x,t)|\leq\emptyset\}\emptyset>0B(t)=\{x,|s(x,t)|\leq\emptyset\} \qquad \emptyset>0 \qquad (3)$$

$$\forall t\geq 0,|x\hat{}i\,(t)|\leq[\![2\lambda]\!]\hat{}i\,\varepsilon, \quad i=0,\ldots\ldots\ldots(n-1) \qquad (4)$$

Where ∅ is boundary layer thickness, ε is tracking precision.

3.3. Selection of Sliding Mode Control over PID control Technique:

PID control technique is one of the most popular and frequently used linear control techniques around the world. But, in the case of microgrid applications, to retain the desired stability albeit the negative incremental load characteristics of CPL, it has been creating some inconveniences due to the lack of consistency of accuracy. Unlike the PID controller, the sliding mode control technique has been developed into the preferable choice to researchers because of its success in practical cases, desired consistency, and straight forward firmware implementation. Besides that, the sliding mode control technique generates discontinuous on/off signals that necessarily force the system to slide along the desired system's behavior. An SMC controller utilizes a discrete sliding decision rule to retain the desired output. According to this, the system, adopting SMC technique, flows through both continuous and discrete modes. By this way, it demonstrates a hybrid feedback configuration in practice. Sliding mode control technique has a number of advantages over the conventional proportional- integral differential (PID) control technique. Hence, in this paper, the sliding mode control technique has been adopted to improve the stability of the microgrid system in the presence of CPL load. The advantages of the SMC control technique are listed below to compare between these two techniques.

- Characteristically, the microgrid system is significantly nonlinear with the time-varying parameters as well as with the system uncertainties. Hence, using PID control technique may hamper system stability due to the possible over linearization of the system. On the other hand, an SMC controller doesn't ignore the system nonlinearity during controller design.
- The efficiency of the entire system depends cardinally on the loading condition. In the case of modeling imprecision, the SMC controller offers a systematic way to the complication of retaining stability as well as the desired consistent performance.
- The sliding mode control technique is easy to implement. It requires short computational and numerical algorithms to implement in the microcontroller. It is readily compatible with the standard communication protocol such as Ethernet/IP, RS-232, and the Modbus.

- In the case of harsh industrial environments, where stability, as well as high performance, is required despite the presence of high nonlinearity, the lifetime of the hardware components can be reduced considerably in the application of PID controller. Unlike PID control technique, SMC offers significantly less equipment and maintenance cost.
- Comparing to PID control technique, SMC offers robust performance against the parametric variations and any disturbance and better response time to retain microgrid stability.

But, in microgrid applications, the main reason for choosing SMC over PID control technique is its robustness against parametric variation and its faster response in solving instability problems.

3.4. Controller Design:

Two steps have to be followed according to the controller design procedure. Initially, it is required to select a feedback control law u to verify the sliding condition. Nevertheless, the control law has to be discontinuous across s (t) to account for the existence of the modeling imprecision as well as of perturbations. As the consequence of the imperfection of associated control switching, it contributes to chattering (see figure 10). In practice, chattering is absolutely undesirable for the system, since this requires a special control scheme. Besides that, it may introduce high-frequency dynamics that was neglected in the case of modeling purpose. After that, in the next step, the discontinuous control law u is to be suitably smoothed to attain an optimal condition in the course of the trade-off between the control bandwidth and tracking precision [32]. Therefore, the first step assures the desired robustness for the parametric uncertainty as well as perturbations, and the second step offers robustness to the high-frequency unmodeled dynamics. The illustrated design steps of the SMC controller are discussed for the microgrid system [33]. Here, we are presenting the modified controller model of microgrid systems to implement the storage-based virtual impedance stabilization technique using SMC controller.

4. Robustness analysis of SMC

Here, the control objectives/desired output of the proposed

Y1= VdC ≈ Vd ≈ 480 Volt
Y2 = VqC ≈ Vq ≈ (as low as possible) Volt

The general form of a system which is affine in the control(s) is given by equation (5) [34]:

$$\dot{x} = f(x) + g(x)u \tag{5}$$

4.1. Sliding Mode Controller, Robustness against parametric uncertainties:

We can rewrite our state space model equation in below (6)

$$\begin{bmatrix} \dot{x_1} \\ \dot{x_2} \\ \dot{x_3} \\ \dot{x_4} \\ \dot{x_5} \\ \dot{x_6} \end{bmatrix} = \begin{bmatrix} \omega x_2 - \frac{R_1}{L_1}x_1 - \frac{x_3}{L_1} \\ -\omega x_1 - \frac{R_1}{L_1}x_2 - \frac{x_4}{L_1} \\ \omega x_4 + \frac{1}{C}x_1 - \frac{1}{C}\frac{P_O}{x_3} - \frac{1}{C}x_5 \\ -\omega x_3 + \frac{1}{C}x_2 - \frac{1}{C}\frac{Q_O}{x_4} - \frac{1}{C}x_6 \\ \omega x_6 + \frac{1}{L}x_3 - \frac{R}{L}x_5 \\ -\omega x_5 + \frac{1}{L}x_4 - \frac{R}{L}x_6 \end{bmatrix} + \begin{bmatrix} 0 \\ 0 \\ -\frac{1}{C}u_1 \\ -\frac{1}{C}u_2 \\ 0 \\ 0 \end{bmatrix} + \begin{bmatrix} \frac{r_1}{L_1} \\ \frac{r_2}{L_1} \\ 0 \\ 0 \\ 0 \\ 0 \end{bmatrix} \tag{6}$$

Where, r_1 and r_2 are unknown parameters that satisfy $r_1 \leq \delta_{r1}$ and $r_2 \leq \delta_{r2}$ for some known bounds δ_{r1} and δ_{r2}. Our goal is to regulate the output active voltage $x_3$and reactive voltage x_4 by designing the control laws u_1 and u_2 respectively. As $x_3$and $x_4$are related to r_1 and r_2 through $x_1$and x_2 respectively. So, x_1 and x_2 are also unknown parameters those satisfy $\Delta x_1 \leq \delta_{x1}$ and $\Delta x_2 \leq \delta_{x2}$ for some known bounds δ_{x1} and δ_{x2}. We will design sliding mode control input, u_1 in the first attempt and then we will follow the similar method to design another control inputu_2.

To make the integral controller, let

$$e_1 = \int (x_3 - x_{3d})dt \tag{7}$$

$$e_2 = \dot{e}_1 = x_3 - x_{3d} \tag{8}$$

$$\dot{e}_2 = \dot{x}_3 - \dot{x}_{3d} = f_3(x) + g_3(x)u_1 - \dot{x}_{3d} \tag{9}$$

Expanding $f_3(x)$ and $g_3(x)$

$$\dot{e}_2 = \omega x_4 + \frac{1}{c}x_1 - \frac{1}{c}\frac{P_0}{x_3} - \frac{1}{c}x_5 - \frac{1}{c}u_1 - \dot{x}_{3d} \tag{10}$$

Let the sliding surface be

$$s = e_1 + e_2$$

Then, its derivative will be

$$\dot{s} = \dot{e}_1 + \dot{e}_2$$

$$\dot{s} = e_2 + (\omega x_4 + \frac{1}{c}x_1 - \frac{1}{c}\frac{P_0}{x_3} - \frac{1}{c}x_5 - \frac{1}{c}u_1 - \dot{x}_{3d})$$

The state $x_1$is unknown, then we can represent the uncertainty as $x_1 = \hat{x}_1 + \Delta x_1$ and

$$\left\|\frac{1}{c}\Delta x_1\right\| \leq \frac{1}{c}\delta_{x1} = e_2 + (-\frac{1}{c}x_5 - \dot{x}_{3d} - \frac{1}{c}\frac{P_0}{x_3} + \omega x_4 + \frac{1}{c}\hat{x}_1 + \frac{1}{c}\Delta x_1 - \frac{1}{c}u_1) \tag{11}$$

Let this be the Lyapunov candidate function

$$\mathrm{V} = \frac{1}{2}s^2$$

$$\dot{\mathrm{V}} = s\dot{s} = s(e_2 + (-\frac{1}{c}x_5 - \dot{x}_{3d} - \frac{1}{c}\frac{P_0}{x_3} + \omega x_4 + \frac{1}{c}\hat{x}_1 + \frac{1}{c}\Delta x_1 - \frac{1}{c}u_1) \tag{12}$$

We use u_1 as

$$u_1 = -c[-e_2 + \frac{1}{c}x_5 + \dot{x}_{3d} + \frac{1}{c}\frac{P_0}{x_3} - \omega x_4 - \frac{1}{c}\hat{x}_1 + v] \tag{13}$$

Then, we can obtain

$$\dot{\mathrm{V}} = s(\frac{1}{c}\Delta x_1 + v)$$

Considering $\left\|\frac{1}{c}\Delta x_1\right\| \leq \frac{1}{c}\delta_{x1}$, the following discontinuous control, v, will make $\dot{\mathrm{V}}$ to be negative, and consequently, guarantee stability

$$v = -\frac{1}{c}\delta_{x1}sat\left(\frac{s}{\varepsilon}\right); \qquad \varepsilon > 0$$

Totally, the control input is

$$u_1 = -c[-e_2 + \frac{1}{c}x_5 + \dot{x}_{3d} + \frac{1}{c}\frac{P_0}{x_3} - \omega x_4 - \frac{1}{c}\hat{x}_1 - \frac{1}{c}\delta_{x1}sat\left(\frac{s}{\varepsilon}\right)] \tag{14}$$

Likeu_1, let

$$e_3 = \int (x_4 - x_{4d})dt$$

$$e_4 = \dot{e}_3 = x_4 - x_{4d} \tag{15}$$

$$\dot{e}_4 = \dot{x}_4 - \dot{x}_{4d} = f_4(x) + g_4(x)u_2 - \dot{x}_{4d} \tag{16}$$

Expanding $f_4(x)$ and $g_4(x)$

$$\dot{e}_4 = -\omega x_3 + \frac{1}{c}x_2 - \frac{1}{c}\frac{Q_0}{x_4} - \frac{1}{c}x_6 - \frac{1}{c}u_2 - \dot{x}_{4d} \quad (17)$$

Let, the sliding surface be

$$s = e_3 + e_4$$

$$\dot{s} = \dot{e}_1 + \dot{e}_2$$

Then, its derivative will be

$$\dot{s} = \dot{e}_3 + \dot{e}_4$$

$$\dot{s} = e_4 + (-\omega x_3 + \frac{1}{c}x_2 - \frac{1}{c}\frac{Q_0}{x_4} - \frac{1}{c}x_6 - \frac{1}{c}u_2 - \dot{x}_{4d})$$

The state x_2 is unknown, then we can represent the uncertainty as $x_2 = \hat{x}_2 + \Delta x_2$ and

$$\left\|\frac{1}{c}\Delta x_2\right\| \le \frac{1}{c}\delta_{x2} = e_4 + (-\omega x_3 + \frac{1}{c}\hat{x}_2 - \frac{1}{c}\frac{Q_0}{x_4} - \frac{1}{c}x_6 - \dot{x}_{4d} + \frac{1}{c}\Delta x_2 - \frac{1}{c}u_2) \quad (18)$$

Let this be the Lyapunov candidate function

$$\mathrm{V} = \frac{1}{2}s^2$$

$$\dot{\mathrm{V}} = s\dot{s} = s(e_4 + \left(-\omega x_3 + \frac{1}{c}\hat{x}_2 - \frac{1}{c}\frac{Q_0}{x_4} - \frac{1}{c}x_6 - \dot{x}_{4d} + \frac{1}{c}\Delta x_2 - \frac{1}{c}u_2\right))$$

We use u_2

$$u_2 = -c[-e_4 + \omega x_3 - \frac{1}{c}\hat{x}_2 + \frac{1}{c}\frac{Q_0}{x_4} + \frac{1}{c}x_6 + \dot{x}_{4d} + v] \quad (19)$$

Then, we can obtain

$$\dot{\mathrm{V}} = s(\frac{1}{c}\Delta x_2 + v)$$

Considering $\left\|\frac{1}{c}\Delta x_2\right\| \le \frac{1}{c}\delta_{x2}$, the following discontinuous control, v, will make $\dot{\mathrm{V}}$ to be negative, and consequently, guarantee stability

$$v = -\frac{1}{c}\delta_{x2}sat\left(\frac{s}{\varepsilon}\right); \qquad \varepsilon > 0$$

Totally, the control input is

$$u_2 = -c[-e_4 + \omega x_3 - \frac{1}{c}\hat{x}_2 + \frac{1}{c}\frac{Q_0}{x_4} + \frac{1}{c}x_6 + \dot{x}_{4d} - \frac{1}{c}\delta_{x2}sat\left(\frac{s}{\varepsilon}\right)] \quad (20)$$

4.2. Sliding Mode Controller Robustness against parametric uncertainties, frequency variations and additive white Gaussian Noise (AWGN):

In this section, we will enhance the robustness by introducing the white noise rejection method. From the last section, we can see that we have to measure just two states as all other states are replaced by their bounds. These two parameters are x_3 and x_5 for $u_1$and, x_4 and x_6 foru_2. As we know that multiplicative noise does not affect the stability of the system, so we will only consider additive noise. Let, the disturbances added to x_3,x_4, x_5 and x_6 be n_3, n_4, n_5 and n_6. Although all the noises; n_3, n_4, n_5 and n_6 are white, let their maximum possible value be δ_{n3}, δ_{n4}, δ_{n5} and δ_{n6} respectively.

Using the similar method as discussed in the last section, let

$$e_1 = \int(x_3 - x_{3d})dt$$

$$e_2 = \dot{e}_1 = x_3 - x_{3d}$$

$$\dot{e}_2 = \dot{x}_3 - \dot{x}_{3d} = f_3(x) + g_3(x)u_1 - \dot{x}_{3d}$$

Expanding $f_3(x)$ and $g_3(x)$

$$\dot{e}_2 = \omega x_4 + \frac{1}{c}x_1 - \frac{1}{c}\frac{P_0}{x_3} - \frac{1}{c}x_5 - \frac{1}{c}u_1 - \dot{x}_{3d} \tag{21}$$

Let, the sliding surface be

$$s = e_1 + e_2$$

After differentiating and adding the noises and uncertainties

$$\dot{s} = e_2 + n_3 + ((\omega + \Delta\omega)(x_4+n_4) + \frac{1}{c}(\hat{x}_1 + \Delta x_1) - \frac{1}{c}(\frac{P_0}{x_3} + d_P) - \frac{1}{c}(x_5 + n_5) - \frac{1}{c}u_1 - \dot{x}_{3d}) \tag{22}$$

Where
$d_P = \Delta_P / n_3$ And $\Delta_P$represents the uncertainties of P_0. This summarizes the variation on the CPL power term as current. Then we can represent the total parametric uncertainty and noises as

$$\mathrm{d} = n_3+\Delta\omega n_4+\Delta\omega x_4 + \omega n_4 + \frac{1}{c}\Delta x_1 - \frac{1}{c}n_5 - \frac{1}{c}d_P; \quad \|\mathrm{d}\| \le dmax$$

Where $dmax$ is the bound of the total disturbance d.

$$dmax = \frac{1}{c}\delta_{x1} + \delta_{n3} + \delta_\omega\delta_{n4}+\delta_\omega\delta_{x4} + \omega\delta_{n4} - \frac{1}{c}\delta_{n5} - \frac{1}{c}\delta_P / \delta_{x3} \tag{23}$$

Then

$$\dot{s} = e_2 - \frac{1}{c}x_5 - \dot{x}_{3d}+\omega x_4 + \frac{1}{c}\hat{x}_1 - \frac{1}{c}\frac{P_0}{x_3} - \frac{1}{c}u_1 + d$$

Let this be the Lyapunov candidate function

$$\mathrm{V} = \frac{1}{2}s^2$$

$$\dot{\mathrm{V}} = s\dot{s} = s(e_2 - \frac{1}{c}x_5 - \dot{x}_{3d}+\omega x_4 + \frac{1}{c}\hat{x}_1 - \frac{1}{c}\frac{P_0}{x_3} - \frac{1}{c}u_1 + d) \tag{24}$$

We use u_1

$$u_1 = -c[-e_2 + \frac{1}{c}x_5 + \dot{x}_{3d}-\omega x_4 - \frac{1}{c}\hat{x}_1 + \frac{1}{c}\frac{P_0}{x_3} + v] \tag{25}$$

Then, we can obtain

$$\dot{\mathrm{V}} = s(d + v)$$

Considering $\|\mathrm{d}\| \le dmax$, the following discontinuous control, v, will make $\dot{\mathrm{V}}$ to be negative, and consequently, guarantee stability

$$v = -dmaxsat\left(\frac{s}{\varepsilon}\right); \qquad \varepsilon > 0$$

Totally, the control input is

$$u_1 = -c[-e_2 + \frac{1}{c}x_5 + \dot{x}_{3d} + \frac{1}{c}\frac{P_0}{x_3} - \omega x_4 - \frac{1}{c}\hat{x}_1 - dmaxsat\left(\frac{s}{\varepsilon}\right)] \tag{26}$$

Similar analysis is also shown here for u_2, let

$$\mathrm{e}_3 = \int(\mathrm{x}_4 - \mathrm{x}_{4\mathrm{d}})\mathrm{dt}$$

$$\mathrm{e}_4 = \dot{\mathrm{e}}_3 = \mathrm{x}_4 - \mathrm{x}_{4\mathrm{d}}$$

$$\dot{\mathrm{e}}_4 = \dot{\mathrm{x}}_4 - \dot{\mathrm{x}}_{4\mathrm{d}} = \mathrm{f}_4(\mathrm{x}) + \mathrm{g}_4(\mathrm{x})\mathrm{u}_2 - \dot{\mathrm{x}}_{4\mathrm{d}}$$

Expanding $\mathrm{f}_4(\mathrm{x})$ and $\mathrm{g}_4(\mathrm{x})$

$$\dot{\mathrm{e}}_4 = -\omega\mathrm{x}_3 + \frac{1}{\mathrm{c}}\mathrm{x}_2 - \frac{1}{\mathrm{c}}\frac{\mathrm{Q}_0}{\mathrm{x}_4} - \frac{1}{\mathrm{c}}\mathrm{x}_6 - \frac{1}{\mathrm{c}}\mathrm{u}_2 - \dot{\mathrm{x}}_{4\mathrm{d}} \tag{27}$$

Let, the sliding surface be

$$\mathrm{s} = \mathrm{e}_3 + \mathrm{e}_4$$

After differentiating and adding the noises and uncertainties

$$\dot{s} = e_4 + n_4 + \begin{pmatrix} -(\omega + \Delta\omega)(x_3 + n_3) + \frac{1}{c}(\hat{x}_2 + \Delta x_2) \\ -\frac{1}{c}(\frac{Q_0}{x_4} + d_Q) - \frac{1}{c}(x_6 + n_6) - \frac{1}{c}u_2 - \dot{x}_{4d} \end{pmatrix} \quad (28)$$

Where
$d_Q = \Delta_Q / n_4$ And Δ_Q represents the uncertainties of Q_0. This summarizes the variation on the CPL power term as current. Then we can represent the total parametric uncertainty and noises as

$$d = n_4 - \omega n_3 - \Delta\omega n_3 - \Delta\omega x_3 + \frac{1}{c}\Delta x_2 - \frac{1}{c}n_6 - \frac{1}{c}d_Q$$

$$\|d\| \leq dmax$$

Where max is the bound of the total disturbance d.

$$dmax = \frac{1}{c}\delta_{x2} - \delta_\omega\delta_{x3} - \delta_\omega\delta_{n3} - \omega\delta_{n3} + \delta_{n4} - \frac{1}{c}\delta_{n6} - \frac{1}{c}\delta_Q / \delta_{x4} \quad (29)$$

Then

$$\dot{s} = e_3 - \frac{1}{c}x_6 - \dot{x}_{4d} + \omega x_3 + \frac{1}{c}\hat{x}_2 - \frac{1}{c}\frac{Q_0}{x_4} - \frac{1}{c}u_2 + d$$

Let this be the Lyapunov candidate function

$$V = \frac{1}{2}s^2$$

$$\dot{V} = s\dot{s} = s(e_3 - \frac{1}{c}x_6 - \dot{x}_{4d} + \omega x_3 + \frac{1}{c}\hat{x}_2 - \frac{1}{c}\frac{Q_0}{x_4} - \frac{1}{c}u_2 + d) \quad (30)$$

We use u_2

$$u_2 = -c[-e_3 + \frac{1}{c}x_6 + \dot{x}_{4d} - \omega x_3 - \frac{1}{c}\hat{x}_2 + \frac{1}{c}\frac{Q_0}{x_4} + v] \quad (31)$$

Then, we can obtain

$$\dot{V} = s(d + v)$$

Considering $\|d\| \leq dmax$, the following discontinuous
Control, v, will make $\dot{V}$ to be negative, and consequently, guarantee stability $v = -dmax sat\left(\frac{s}{\varepsilon}\right)$;
$\varepsilon > 0$
Totally, the control input is

$$u_2 = -c[-e_3 + \frac{1}{c}x_6 + \dot{x}_{4d} - \omega x_3 - \frac{1}{c}\hat{x}_2 + \frac{1}{c}\frac{Q_0}{x_4} - dmax sat\left(\frac{s}{\varepsilon}\right) \quad (32)$$

5. Results

In this paper, a sliding mode controller (SMC) has been selected by a PID controller due to considerably better performance. In figure 11, performance comparisons between PID (blue colored) and SMC (red colored) have been shown in the case of (a) real axis output voltage and (b) reactive axis output voltage for nonlinear system application. It has been seen that the PID controller experienced initial chattering rather than stabilized d-axis output voltage in face of nonlinearity. In the case of the q-axis output voltage, the PID controller doesn't experience appreciable stabilization, but continuous chattering. On the other hand, the sliding mode controller experienced quick and firm output voltage stabilization in face of microgrid nonlinearity. After that, performance comparison between PID and SMC has been presented at figure 12 in the case of (a) real axis output voltage and (b) reactive axis output voltage considering parametric uncertainties. Here, it is evident that the chattering range of the PID controller is considerably more than that of the sliding mode controller. Hence, in the case of parametric uncertainties, SMC shows significantly better performance than PID controller. Then, in figure 13, performance comparison between PID and SMC has been illustrated in the case of (a) real axis output voltage and (b) reactive axis output voltage considering noise rejection. Here, the Sliding Mode Controller handled the instability issue better. Hence, to improve the microgrid stability in the presence of dense CPL, the sliding mode controller

is chosen over the PID controller in load side compensation technique. Here, now, the sliding mode controller simulation platform is presented in figure 14.

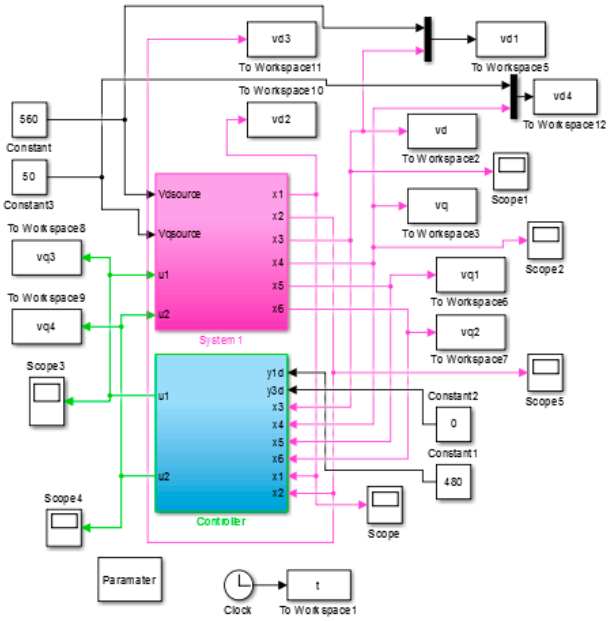

Figure 14: Matlab/Simulink schematic model of sliding mode control of microgrid.

Performance comparisons between robustness analysis against parametric variation and robustness analysis against parametric uncertainties, frequency variation and additive Gaussian noise using SMC control technique based on Performance comparison between robustness analysis against parametric variation and robustness analysis against parametric uncertainties, frequency variation and additive Gaussian noise using SMC control technique based on boundary condition have been analyzed here in figure 15 and 16.

For robustness analysis, we have to take a Lyapunov function and put the feedback system in it. In this case, we will perturb the unknown parameters. Here, we can also define some performance comparison between robustness analysis against parametric variation and robustness analysis against parametric uncertainties, frequency variation and additive Gaussian noise using SMC control technique based on boundary condition have been analyzed here in figure 15 and 16.

Here, we can also define some numerical values of bounds and the perturbed parameters for robustness analysis.

For u_1

Let, $\omega = 60\text{Hz}, x_3 = 600\text{V}, x_4 = 10\text{V}$, $\Delta x_1 = 200\text{A}$, $\Delta x_2 = 200\text{A}$ $n_3 = 50\text{V}$, $n_4 = 50\text{V}$, $n_5 = 30A, n_6 = 30A$, $\Delta\omega = 10\text{Hz}$, $d_P = 50\text{A}$, and $d_Q = 20\text{A}$. Also, we have the numerical value of bounds; $\delta_{x1} = 4000\text{A}$, $\delta_{x4} = 100\text{V}$, $\delta_\omega = 70\text{Hz}$, $\delta_P = 30\text{kW}$, $\delta_Q = 20\text{Var}, \delta_{n3} = \delta_{n4} = \delta_{n5} = \delta_{n6} = 100A$, $\rho_{x3} = 200\text{V}$, and $\varepsilon = 100$.

$$\dot{V} = s(d+v) = s(n_3 + \Delta\omega n_4 + \Delta\omega x_4 + \omega n_4 + \frac{1}{c}\Delta x_1 - \frac{1}{c}n_5 - \frac{1}{c}d_P - \left[\frac{1}{c}\delta_{x1} + \delta_{n3} + \delta_\omega\delta_{n4} + \delta_\omega\delta_{x4} + \omega\delta_{n4} - \frac{1}{c}\delta_{n5} - \frac{\delta_P}{C\delta_{x3}}\right] sat\left(\frac{s}{\varepsilon}\right)) \quad (33)$$

$$\dot{V} = s\left[50 + (10)(50) + (10)(10) + (60)(50) + \frac{1}{c}(200) - \frac{1}{c}(30) - \frac{1}{c}(50) - \left[\frac{1}{c}4000 + 100 + (70)(100) + (70)(100) + (65)(100) - \frac{1}{c}100 - \frac{1}{c}\left(\frac{30000}{200}\right)\right] sat\left(\frac{s}{100}\right)\right] \quad (34)$$

$$\dot{V} = s\left[18.004 \times 10^6 - [375.021 \times 10^6] sat\left(\frac{s}{100}\right)\right] \quad (35)$$

Now, if s is either positive or negative, we will get $\dot{V} \leq 0$.

Preprints (www.preprints.org) | NOT PEER-REVIEWED | Posted: 18 May 2017 doi:10.20944/preprints201705.0137.v1

Peer-reviewed version available at Energies 2017, 10, 1086; doi:10.3390/en10081086

For u_2

$$\dot{V} = s(d+v) = s\Big(\Big[n_4 - \omega n_3 - \Delta\omega n_3 - \Delta\omega x_3 + \frac{1}{c}\Delta x_2 - \frac{1}{c}n_6 - \frac{1}{c}d_Q - \Big[\frac{1}{c}\delta_{x2} + \delta_{n4} - \frac{1}{c}\delta_{n6} - \delta_\omega\delta_{x3} - \delta_\omega\delta_{n3} - \omega\delta_{n3} - \delta_Q/\delta_{x4}\Big] sat\left(\frac{s}{100}\right)\Big] \quad (36)$$

$$\dot{V} = s\Big[50 - (60)(50) - (10)(600) - (10)(50) + \frac{1}{c}(200) - \frac{1}{c}(30) - \frac{1}{c}(20) - \Big[\frac{1}{c}1000 + 100 - (70)(1000) - (70)(100) - (65)(100) - \frac{1}{c}100 - \frac{1}{c}\left(\frac{20}{1}\right)\Big] sat\left(\frac{s}{100}\right)\Big] \quad (37)$$

$$\dot{V} = s\Big[14.99 \times 10^6 - [79.916 \times 10^6] sat\left(\frac{s}{100}\right)\Big] \quad (38)$$

Now, if s is either positive or negative, we will get $\dot{V} \leq 0$
So, as a derivative of a Lyapunov function is negative, our system will remain stable even in the case of perturbing.

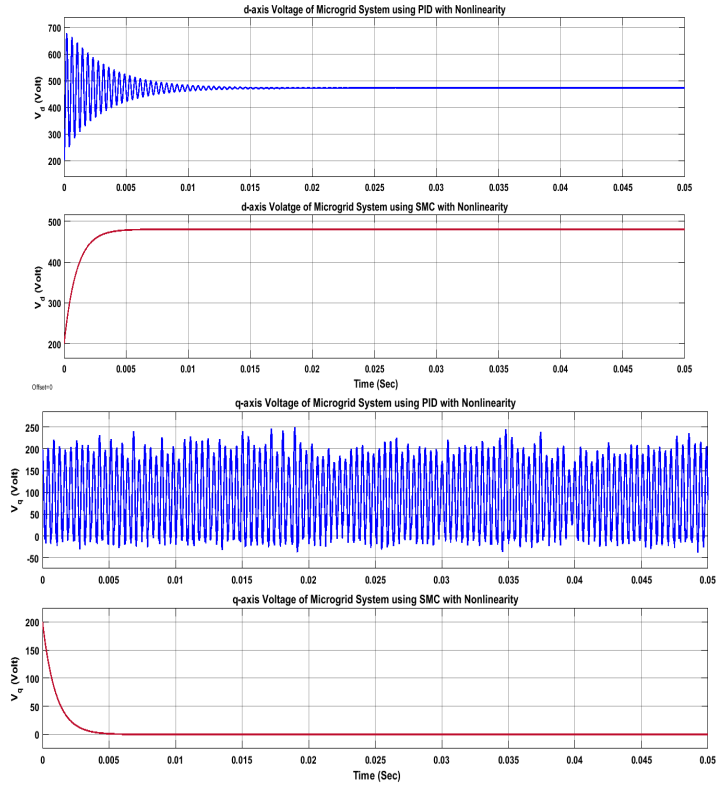

Figure 11: Performance comparison between PID (blue colored) and SMC (red colored) in the case of (a) real axis output voltage (Vd) and (b) reactive axis output voltage (Vq) for nonlinear system application.

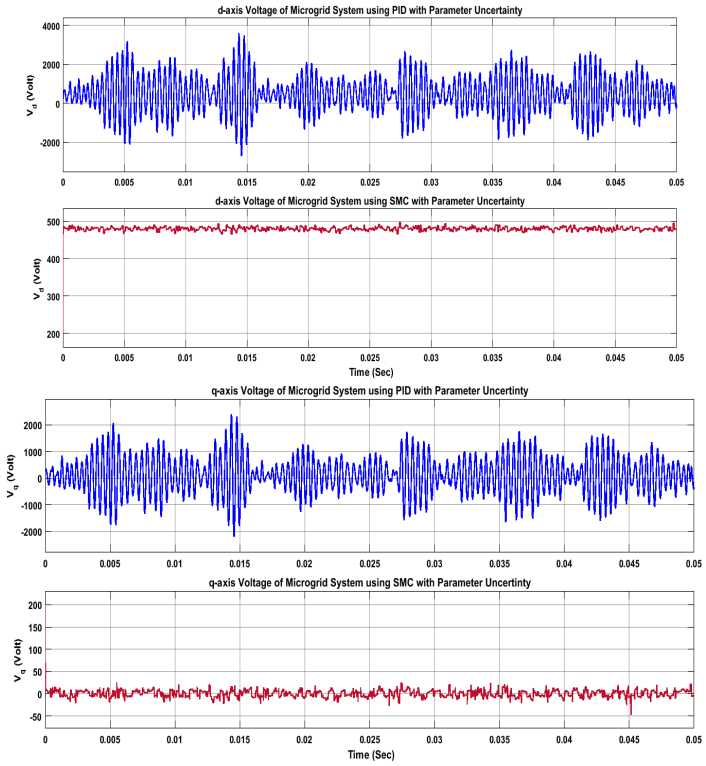

Figure 12: Performance comparison between PID (blue colored) and SMC (red colored) in the case of (a) real axis output voltage (Vd) and (b) reactive axis output voltage (Vq) considering parametric uncertainties.

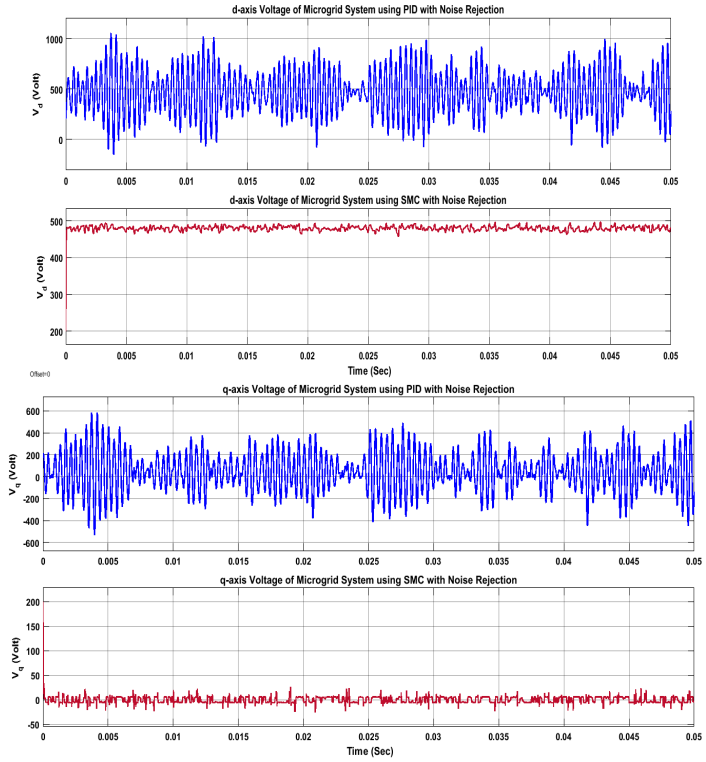

Figure 13: Performance comparison between PID (blue colored) and SMC (red colored) in the case of (a) real axis output voltage (Vd) and (b) reactive axis output voltage (Vq) considering noise rejection.

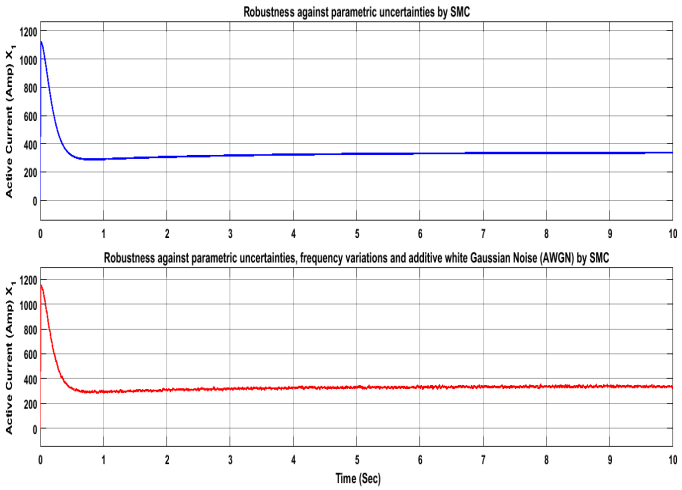

(a)

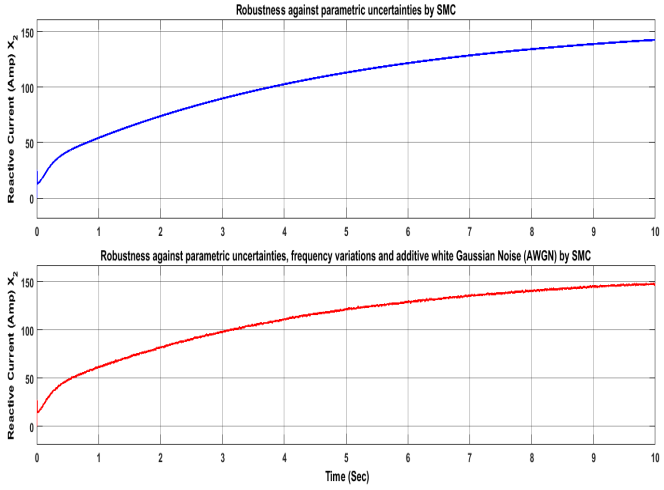

(b)

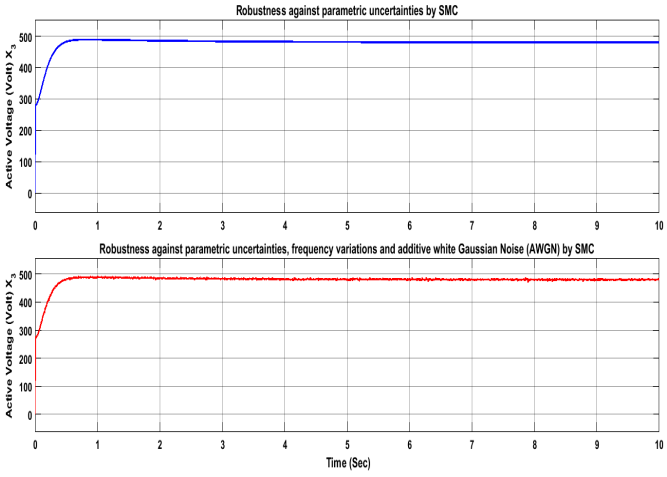

(c)

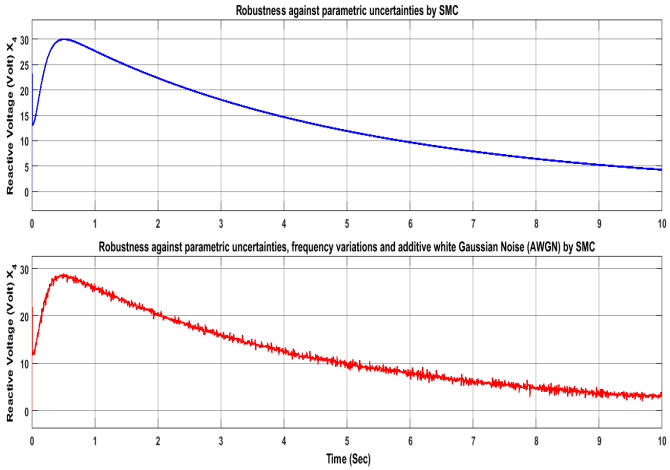

(d)

Figure 15: (a) d-axis current comparison, (b) q-axis current comparison, (c) d-axis bus voltage comparison, and (d) q-axis bus voltage comparison, between robustness analysis against parametric variation and robustness analysis against parametric uncertainties, frequency variation and additive Gaussian noise using SMC control technique based on boundary conditions.

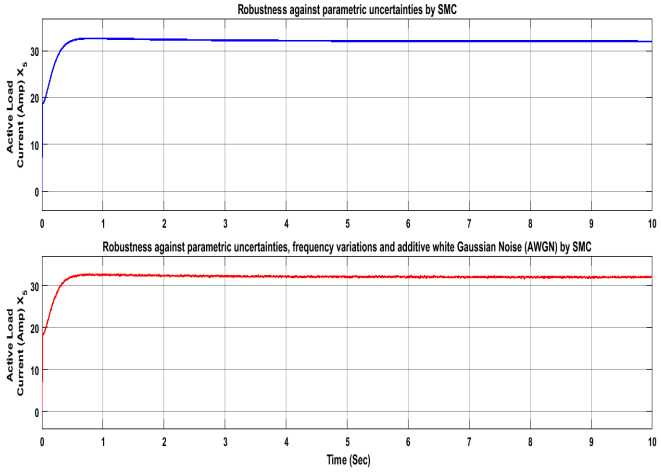

(a)

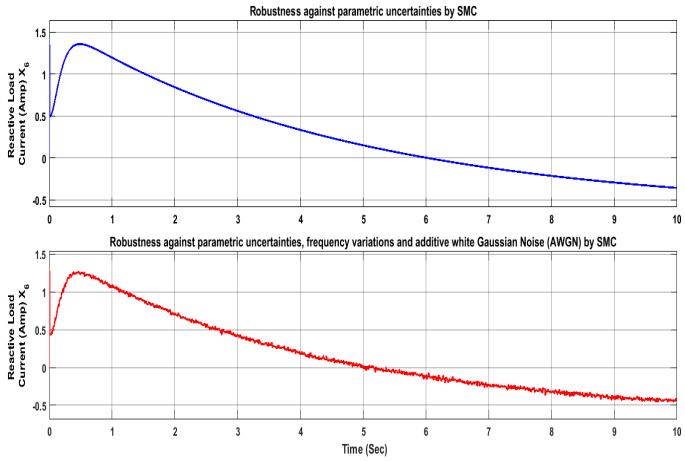

(b)

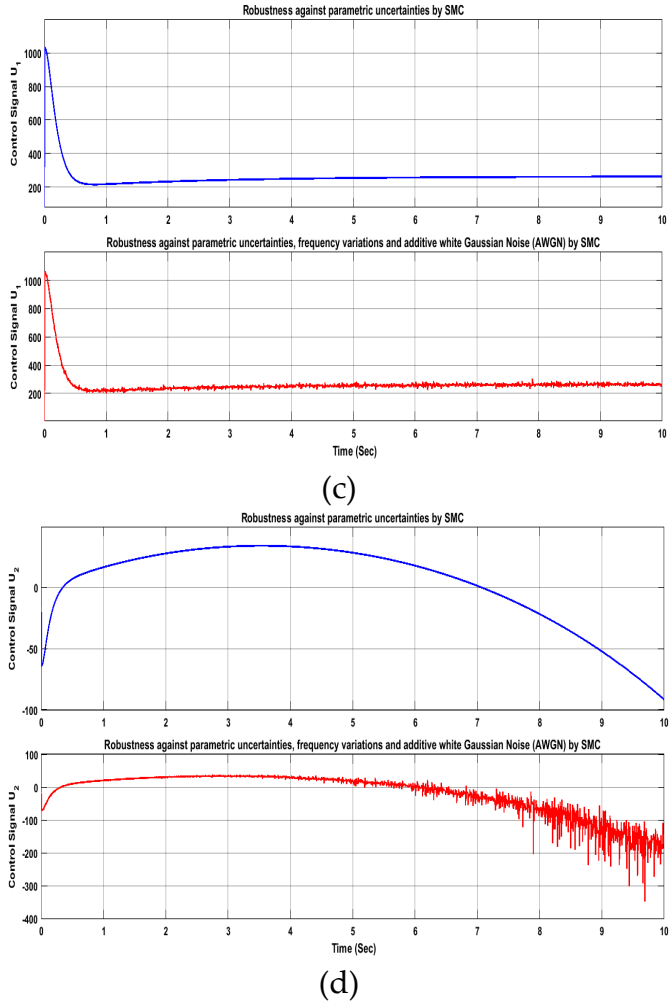

Figure 16: (a) d-axis current (CVL load) comparison, (b) q-axis current (CVL load) comparison, (c) d-axis current compensation (d-axis control signal) comparison, and (d) q-axis current compensation (q-axis control signal) comparison, between robustness analysis against parametric variation and robustness analysis against parametric uncertainties, frequency variation and additive Gaussian noise using SMC control technique based on boundary condition.

6. Conclusion

Though microgrid systems have several advantages over the utility grid system, to adopt this system for mass electrification is cumbersome due to the CPL instability. To improve the stability scenario of microgrid system, in this paper, load side compensation technique has been adopted. Besides the discussion about the previous research work on sliding mode control technique, a sliding mode controller has been developed for microgrids with constant power load to assure control objectives/desired output. Initially, constant power load instability has been presented with necessary illustration. After that, the Sliding Mode Control (SMC) technique has been introduced in this paper. Apart from that, the control principle of SMC, chattering, chattering reduction, advantages of SMC, controller design, and the control objectives have been delineated with necessary equations and depictions. Then, the robustness analysis of SMC has been presented in this letter. After that, the results and simulations have been illustrated in the case of a number of system parameters between robustness analysis against parametric variation and robustness analysis against parametric uncertainties, frequency variation and additive Gaussian noise using SMC control technique based on boundary condition. Later, the performance of the PID and the sliding mode controller has been compared in case of nonlinearity, parameter uncertainties, and noise

rejection to justify the selection of Sliding Mode controller over PID controller. To verify the performance of this approach, the simulation results have been demonstrated on a virtual platform such as MATLAB/Simulink.

Acknowledgments: No source of funding for this research project.

Author Contributions: All authors involved equally in the development of the proposed research concept with the complete development from the base toward theoretical prediction and the concept of investigated microgrids with sliding mode controller. Further, the numerical simulation software implementation tasks were carried out by Eklas Hossain and Sanjeevikumar Padmanaban, validated the proposal with the expected outcomes and theoretical background. Ron Perez and Pierluigi Siano shared their expertise in the microgrids for its further quality in depiction and validation of the proposal. All authors involved and formatted the article for its full research decimation.

Conflicts of Interest: The authors declare no conflict of interest.

References

1. Eklas Hossain, Ersan Kabalci, Ramazan Bayindir and Ronald Perez "Microgrid testbeds around the world: State of art", Energy Conversion and Management, vol.86, pp. 132–153.
2. V.A. Evangelopoulos, et al., "Optimal operation of smart distribution networks," A review of models, methods and future research, Electr. Power Syst. Res. (2016).
3. Farhan H. Malik, Matti Lehtonen, "A review: Agents in smart grids," Electric Power Systems Research, Vol. 131, pp. 71-79, Feb. 2016.
4. Aushiq Ali Memon, Kimmo Kauhaniemi, "A critical review of AC Microgrid protection issues and available solutions," Electric Power Systems Research, vol. 129, pp. 23-31, Dec. 2016.
5. C.N. Papadimitriou, E.I. Zountouridou, N.D. Hatziargyriou, "Review of hierarchical control in DC microgrids," Electric Power Systems Research, vol. 122, pp. 159-167, May. 2015.
6. Sanchez, S.; Ortega, R.; Griño, R.; Bergna, G.; Molinas, M., "Conditions for Existence of Equilibria of Systems With Constant Power Loads," Circuits and Systems I: Regular Papers, IEEE Transaction, vol. 61, no. 7, pp. 2204,2211, July 2014.
7. Y. Li, K. R. Vannorsdel, A. J. Zirger, M. Norris and D. Maksimovic, "Current Mode Control for Boost Converters With Constant Power Loads," in IEEE Transactions on Circuits and Systems I: Regular Papers, vol. 59, no. 1, pp. 198-206, Jan. 2012.
8. S. Sanchez, R. Ortega, R. Griño, G. Bergna and M. Molinas, "Conditions for Existence of Equilibria of Systems With Constant Power Loads," IEEE Transactions on Circuits and Systems I: Regular Papers, vol. 61, no. 7, pp. 2204-2211, July 2014.
9. N. Barabanov, R. Ortega, R. Griñó and B. Polyak, "On Existence and Stability of Equilibria of Linear Time-Invariant Systems with Constant Power Loads," IEEE Transactions on Circuits and Systems I: Regular Papers, vol. 63, no. 1, pp. 114-121, Jan. 2016.
10. A. Trias and J. L. Marín, "The Holomorphic Embedding Load flow Method for DC Power Systems and Nonlinear DC Circuits," IEEE Transactions on Circuits and Systems I: Regular Papers, vol. 63, no. 2, pp. 322-333, Feb. 2016.
11. M. Wu and D. D. C. Lu, "A Novel Stabilization Method of LC Input Filter With Constant Power Loads Without Load Performance Compromise in DC Microgrids," IEEE Transactions on Industrial Electronics, vol. 62, no. 7, pp. 4552-4562, July 2015.
12. A. Kwasinski and C. N. Onwuchekwa, "Dynamic Behavior and Stabilization of DC Microgrids With Instantaneous Constant-Power Loads," IEEE Transactions on Power Electronics, vol. 26, no. 3, pp. 822-834, March 2011.
13. Huddy, S.R.; Skufca, J.D., "Amplitude Death Solutions for Stabilization of DC Microgrids with Instantaneous Constant-Power Loads," Power Electronics, IEEE Transactions, vol. 28, no. 1, pp. 247, 253, Jan. 2013
14. S. Sanchez and M. Molinas, "Large Signal Stability Analysis at the Common Coupling Point of a DC Microgrid: A Grid Impedance Estimation Approach Based on a Recursive Method," IEEE Transactions on Energy Conversion, vol. 30, no. 1, pp. 122-131, Mar. 2015.

15. Marx, D.; Magne, P.; Nahid-Mobarakeh, B.; Pierfederici, S.; Davat, B., "Large Signal Stability Analysis Tools in DC Power Systems With Constant Power Loads and Variable Power Loads—A Review," Power Electronics, IEEE Transactions, vol. 27, no. 4, pp. 1773,1787, Apr. 2012.
16. Magne, P.; Marx, D.; Nahid-Mobarakeh, B.; Pierfederici, S., "Large-Signal Stabilization of a DC Link Supplying a Constant Power Load Using a Virtual Capacitor: Impact on the Domain of Attraction," Industry Applications, IEEE Transaction, vol. 48, no. 3, pp. 878,887, May-June 2012.
17. Jelani, N.; Molinas, M.; Bolognani, S., "Reactive Power Ancillary Service by Constant Power Loads in Distributed AC Systems," Power Delivery, IEEE Transactions, vol. 28, no. 2, pp. 920,927, Apr. 2013.
18. Singh, S.; Fulwani, D.; Kumar, V., "Robust sliding-mode control of dc/dc boost converter feeding a constant power load," Power Electronics, IET , vol. 8, no. 7, pp. 1230,1237, 2015.
19. A. R. Gautam, S. Singh and D. Fulwani, "DC bus voltage regulation in the presence of constant power load using sliding mode controlled dc-dc Bi-directional converter interfaced storage unit," DC Microgrids (ICDCM), 2015 IEEE First International Conference on, Atlanta, GA, pp. 257-262, 2015.
20. Stramosk, V.; Pagano, D.J., "Nonlinear control of a bidirectional dc-dc converter operating with boost-type Constant-Power Loads," Power Electronics Conference (COBEP), Brazilian, pp. 305,310, 27-31 Oct. 2013.
21. Zeng Liu; Jinjun Liu; Weihan Bao; Yalin Zhao, "Infinity-Norm of Impedance-Based Stability Criterion for Three-Phase AC Distributed Power Systems With Constant Power Loads," Power Electronics, IEEE Transactions on , vol.30, no.6, pp.3030,3043, Jun. 2015.
22. Jelani, N.; Molinas, M.; Bolognani, S., "Reactive Power Ancillary Service by Constant Power Loads in Distributed AC Systems," Power Delivery, IEEE Transactions, vol.28, no.2, pp.920, 927, Apr. 2013.
23. A. Emadi, "Modeling of power electronic loads in AC distribution systems using the generalized State-space averaging method," IEEE Transactions on Industrial Electronics, vol. 51, no. 5, pp. 992-1000, Oct. 2004.
24. Karimipour, D.; Salmasi, F.R., "Stability Analysis of AC Microgrids With Constant Power Loads Based on Popov's Absolute Stability Criterion," Circuits and Systems II: Express Briefs, IEEE Transactions on , vol. 62, no. 7, pp. 696,700, July 2015.
25. S. Jian, "Small-signal methods for AC distributed power systems—A review," IEEE Trans. Power Electron., vol. 24, no. 11, pp. 2545–2554, Nov. 2009.
26. Vilathgamuwa, D.M.; Zhang, X.N.; Jayasinghe, S.D.G.; Bhangu, B.S.; Gajanayake, C.J.; King Jet Tseng, "Virtual resistance based active damping solution for constant power instability in AC microgrids," IECON 2011 - 37th Annual Conference on IEEE Industrial Electronics Society, pp. 3646,3651, 7-10 Nov. 2011.
27. Ganjefar S, Sarajchi M, Mahmoud Hoseini SS. "Teleoperation Systems Design Using Singular Perturbation Method and Sliding Mode Controllers. ASME," J. Dyn. Sys. Meas., Control; vol. 136, no. 6 pp. 051005-051005-8, 2014.
28. H. K. Khalil, Nonlinear Systems, 3rd ed. Upper Saddle River, NJ, USA: Prentice-Hall, 2002.
29. Y.Z. Elhalwagy, M. Tarbouchi, "Fuzzy logic sliding mode control for command guidance law design," ISA Transactions, vol. 43, no. 2, pp. 231-242, Apr. 2004.
30. Torchani, A. Sellami and G. Garcia, "Sliding mode control of saturated systems with norm bounded uncertainty," 2012 16th IEEE Mediterranean Electrotechnical Conference, Yasmine Hammamet, pp. 15-18, 2012.
31. https://theses.lib.vt.edu/theses/available/etd5440202339731121/unrestricted/CHAP4_DOC.pdf
32. D. Wang, Q. Zhang and A. Wang, "Robust nonlinear control design for ionic polymer metal composite based on sliding mode approach," Control (CONTROL), 2014 UKACC International Conference on, Loughborough, 2014, pp. 519-524. doi: 10.1109/CONTROL.2014.6915194
33. Santi, E.; Li, D.; Monti, A.; Stankovic, A.M., "A Geometric Approach to Large-signal Stability of Switching Converters under Sliding Mode Control and Synergetic Control," Power Electronics Specialists Conference, 2005. PESC '05. IEEE 36th, pp.1389, 1395, Jun. 2005.
34. Farrell, Jay A., and Marios M. Polycarpou. "Adaptive approximation based control: unifying neural, fuzzy and traditional adaptive approximation approaches," John Wiley & Sons, Vol. 48, 2006.